CISTER
Research Centre in
Real-Time & Embedded
Computing Systems

Conference Paper

Performance Analysis of a VLC System Applied to a Hospital Environment for IoT-based Smart Patient Monitoring

Benjamín Fernández
Pablo Palacios Játiva
Cesar A. Azurdia Meza
Nicolás Boettcher
David Zabala Blanco
Miguel Gutiérrez Gaitán*
Ismael Soto

*CISTER Research Centre

CISTER-TR-240505

2024/07/17

Performance Analysis of a VLC System Applied to a Hospital Environment for IoT-based Smart Patient Monitoring

Benjamín Fernández, Pablo Palacios Játiva, Cesar A. Azurdia Meza, Nicolás Boettcher, David Zabala Blanco, Miguel Gutiérrez Gaitán*, Ismael Soto

*CISTER Research Centre

Polytechnic Institute of Porto (ISEP P.Porto)

Rua Dr. António Bernardino de Almeida, 431

4200-072 Porto

Portugal

Tel.: +351.22.8340509, Fax: +351.22.8321159

E-mail: benjamin.fernandez2@mail.udp.cl, nicolas.boettcher@mail.udp.cl, dzabala@ucm.cl, mjggt@isep.ipp.pt

https://www.cister-labs.pt

Abstract

This article discusses the deployment of effective communication networks for smart IoT-based smart patient monitoring in medical facilities, advocating for the adoption of Visible Light Communication (VLC) technology. Initially, the physical scenario is analyzed, taking into account factors such as line-of-sight (LOS) and nonline-of-sight (NLOS) channel components. Furthermore, a transmitter is designed to offer a substitute in the event of potential disruptions due to patient motion or loss of line-of-sight elements. The performance of the proposed system is verified under certain performance metrics, such as the Channel Impulse Response (CIR) and the Cumulative Distribution Function (CDF), with respect to power measurements at different points. The results highlight the effects that NLOS rays have on the received data and the received power. Therefore, this study serves as a step towards the development of more sophisticated systems for patient monitoring using enabling technologies such as VLC.

Performance Analysis of a VLC System Applied to a Hospital Environment for IoT-based Smart Patient Monitoring

Benjamín Fernández*, Pablo Palacios Játiva*, Cesar A. Azurdia-Meza†, Nicolás Boettcher*,
David Zabala-Blanco‡, Miguel Gutiérrez Gaitán§¶, Ismael Soto‖
*Universidad Diego Portales, Santiago, Chile, {benjamin.fernandez2, pablo.palacios, nicolas.boettcher}@mail.udp.cl,
†Department of Electrical Engineering, Universidad de Chile, Santiago, Chile, cazurdia@ing.uchile.cl
‡ Universidad Católica del Maule, Chile, dzabala@ucm.cl
§Pontificia Universidad Católica de Chile, Chile, miguel.gutierrez@uc.cl
¶CISTER Research Centre, Portugal, mjggt@isep.ipp.pt
‖Department of Electrical Engineering, Universidad de Santiago de Chile, Santiago, Chile, ismael.soto@usach.cl

2024 14th International Symposium on Communication Systems, Networks and Digital Signal Processing (CSNDSP) | 979-8-3503-4874-3/24/$31.00 ©2024 IEEE | DOI: 10.1109/CSNDSP60683.2024.10636464

Abstract—**This article investigate the deployment of effective communication networks for smart IoT-based smart patient monitoring in medical facilities, advocating for the adoption of Visible Light Communication (VLC) technology. Initially, the physical scenario is analyzed, taking into account factors such as line-of-sight (LOS) and nonline-of-sight (NLOS) channel components. Furthermore, a transmitter is designed to offer a substitute in the event of potential interruptions due to patient motion or loss of line-of-sight elements. The performance of the proposed system is verified under certain performance metrics, such as the Channel Impulse Response (CIR) and the Cumulative Distribution Function (CDF), with respect to power measurements at different points. The results highlight the effects that NLOS rays have on the received data and the received power. Therefore, this study serves as a step towards the development of more sophisticated systems for patient monitoring using enabling technologies such as VLC.**

Index Terms—**E-HEALTH, IoT, optical channels, smart patient monitoring, visible light communication (VLC).**

I. Introduction

Remote patient monitoring is an increasingly common practice in the field of medicine, with growing applications, especially during the COVID-19 pandemic [1]. To satisfy remote monitoring requirements, such as data stability and transmission speed, various technologies and communication media have been used, most of which involve wireless communications between signal transmitters and hubs. These technologies allow wireless measurement and transmission of vital signs such as blood pressure, heart rate, oxygen saturation, and patient temperature. Currently, technologies such as video telemonitoring systems [2] and internet of things (IoT) systems [3], [4] enable wireless and remote monitoring of patients.

Among the advantages provided by wireless communication systems for monitoring patients, we can include increased patient comfort and mobility, improved efficiency in medical care (by reducing the need for manual measurements), flexibility, and scalability, among others. Therefore, it can be said that these technologies contribute to more effective and high-quality medical care. However, these days there are more modern alternatives that allow us to mitigate problems such as RF interference and help to make better use of indoor environment elements, such as hospital lighting. Furthermore, smart health based on the IoT requires low-power, green communication and connectivity. Therefore, visible light communication (VLC) is one of the candidates to meet these requirements.

In this context, VLC technology has emerged as a promising alternative for data transmission between monitoring devices and base stations. This technology uses visible light as the communication medium, which is a complementary and promising option compared to the other options mentioned above for wireless patient monitoring. This communication is achieved by modulating the intensity of light emitted by a light-emitting device called a light-emitting diode (LED) to transmit information. One of its various applications is in data transmission in light-fidelity (Li-Fi) systems, enabling wireless connectivity in an indoor environment through already installed lighting [5], [6].

The application of VLC systems in hospitals is a paradigm that has evolved and has gained greater importance over time. Some research refers to its implementation, as in the article presented in [7], which discusses the use of VLC in hospitals to provide Li-Fi as a type of connection. This article reports on an experimental transmission study in a typical neurosurgery room. In the paper described in [8], E-HEALTH is discussed as an efficient complement to traditional medical care services, and to support its use, the proposal includes the implementation of a VLC system to create a hybrid system to improve indoor hospital applications. In these two mentioned articles, the use of VLC systems is reflected, improving different areas of the hospital to improve established systems or provide better services.

In addition to the previously described use of VLC in hospitals, its application in patient monitoring has also been considered. In the article presented in [9], the use of optical wireless communication (OWC) is described, involving data transmission through infrared communication (IR) and proposing a periodic data scheme to transmit data from multiple patients. The article described in [10] presents a sensor system that uses VLC technology to transmit patient data, such as electrocardiograms, temperature, and photoplethysmography.

Despite the research presented, various crucial aspects regarding the use of VLC in this environment have yet to be evaluated. These aspects may include improvements in transmission rates through encoding methods, consideration of different locations for the optical receiver, potential nonline-of-sight (NLOS) issues that may arise between the transmitter and receiver, or challenges related to data detection when the patient moves the transmitter or if it is obstructed by any object.

This article is intended to contribute to patient monitoring systems in hospitals using VLC technology by addressing potential reflections in a room. It proposes a new type of transmitter designed to accommodate obstacles or patient movements, considering various points where a receiver can be placed. To evaluate the proposed solution in these scenarios, a simulation developed in Matlab software will be performed. The simulation will verify different receiver positions by analyzing the channel impulse response (CIR) and the cumulative distribution function (CDF) of the received powers. This analysis takes into account a certain number of calculated reflections.

The remainder of the paper is organized as follows. Section II introduces the system model, encompassing factors such as optical transmitter, optical receiver, and channel representation. Section III presents the parameter values considered in the simulation, along with the optical receiver locations that will be evaluated. In Section IV, a system performance assessment is conducted through CIR curves and a CDF of received powers to generate an analysis based on the results obtained. Finally, Section V provides the conclusion of the article.

II. System Model

The proposed model comprises two essential elements that facilitate VLC communication for monitoring: the transmitter (LED) and the optical receiver, which consists of a photodiode (PD). The LED is placed on the patient's wrist, alongside an information processing system that gathers the required user data for transmission. The transmitter is designed as a wristband-style instrument, featuring two separate LEDs to maintain continuous communication, even in the event of 180^o rotation of the transmitter. The graphical sketch of the transmitter can be observed in Figure 1.

On the other hand, the receiver's position is analyzed to be located on one side of the room, as close as possible to the patient and pointing towards a corner of the room. This location was adopted to minimize the presence of obstacles in the path of the light beam. However, the existence of various light rays, generated by reflections known as NLOS, must still be considered, as shown in Figure 1.

Regarding the mathematical formulation of the system, based on the conventional wireless communication model, the relationship between the transmitter, receiver, and channel can be described as follows [11], [12]:

$$y = h * x + w, \tag{1}$$

where y is the received signal, h is the impulse response in the optical channel, x is the transmitted signal, and w is the Gaussian noise.

Equation 1 is a simplification of the optical system model. In the case of this manuscript, its adaptation is based on the reference system in Figure 2. The mathematical models of the components of the developed system will be described in the following subsections.

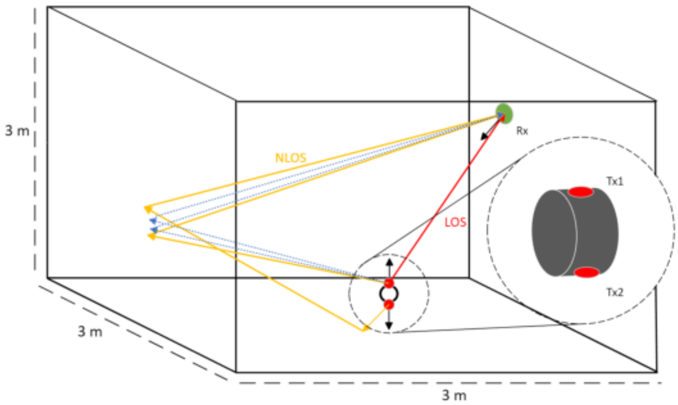

Figure 1. Proposed scenario with the respective applied rays.

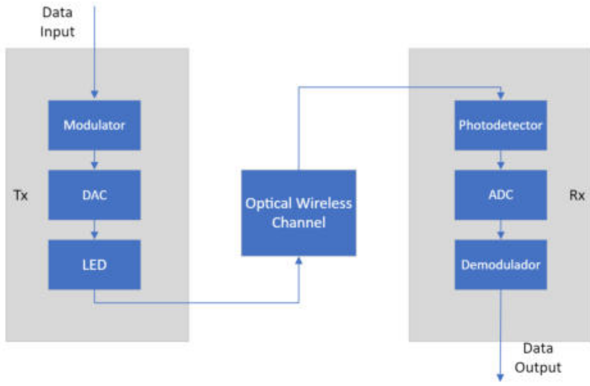

Figure 2. Reference system.

A. Transmitter

The transmitter is the first element of the system and is where the processing of the data to be transmitted takes place. When establishing a sequence of processes, the transmitter block diagram is described in Figure 2. In this scheme, we can observe that the signal is first modulated and will be transmitted by the LED by converting it from digital to analog using the digital analog converter (DAC).

The mathematical model of the transmitter can be represented as [12]:

$$x = \tau\sigma\xi P_a x_a. \tag{2}$$

Various components of equation 2 refer to processes or effects that occur in the transmitter (Tx), where τ is the electro-optical conversion efficiency, σ is the responsivity of the photodetector, ξ is the modulation index of the transmitter, x_a is the electrical signal transmitted by Tx, and P_a is the average optical power at the output of Tx.

B. Channel

The system model implemented in this work considers the effect of the LED transmitting a light signal through an optical channel in a typical indoor environment, taking into account the line-of-sight (LOS) and NLOS components of the channel. Therefore, the base VLC channel model we consider can be expressed by the sum of both components in the following way [11], [13]:

$$h = h_{LOS} + \sum_{i=1}^{I} h_{NLOS_i}, \tag{3}$$

where h_{LOS} is the light beam formed by the line of sightand h_{NLOS} is the sum of all the I reflections that may exist in the scenario.

In the case of the interaction generated by the LOS component, it is simpler and takes into account fewer problems in the environment. Therefore, it is the ideal case. This channel component is modeled based on the Lambertian radiation model, which is shown in the following equation:

$$h_{LOS} = \frac{A}{d^2} R(\varphi) F(\phi) C(\phi) \cdot \cos\phi, \tag{4}$$

where A is the active area of the PD, d is the Euclidean distance between the LED and the PD, ϕ is the angle at which the light impacts the PD, $F(\phi)$ is the gain of the LED's optical filter, $C(\phi)C(\phi)$ is the gain of the concentrator, φ is the irradiance angle, $R(\varphi)$ is the intensity of the LED transmitter.

The function $R(\varphi)$ is defined by the following expression:

$$R(\varphi) = \left[\frac{\eta + 1}{2\pi}\right] \cos^{\eta}\varphi, \tag{5}$$

where η is the Lambertian index, which is defined as:

$$\eta = \log_2(\cos\phi_{1/2})^{-1}, \tag{6}$$

with $\phi_{1/2}$ being half of the angle of incidence of light on PD.

For the NLOS case, our implementation is based on the following expression, which follows the typical Lambertian model of secondary irradiation [14]:

$$h_{NLOS}(t, S, R_x) = \sum_{k=0}^{\infty} h_{NLOS}^{(k)}(t, S, R). \tag{7}$$

This expression is derived from a single origin point, which will be called S, and a destination point on the receiver, which will be called R, represented in a scenario that emulates a room. Therefore, $h_{NLOS}(t, S, R)$ describes the impulse response with k reflections [11], [5].

$$h_{NLOS}(t, S, R_x) = \frac{\eta+1}{2\pi} \sum_{j=1}^{K} \rho_j \cos^{\eta}(\varphi_j) \frac{\cos(\phi)}{d_{Sj}^2} rect\left(\frac{2\phi}{\pi}\right) \times h_{nlos}^{(k-1)}\left(t - \frac{d_{Sj}}{c}, S, R_x\right) \Delta A, \tag{8}$$

where k is the number of reflections, ρ_j is the reflection coefficient of j, d_{Sj} is the distance between j and S, $h_{nlos}^{(k-1)}$ is the impulse response of order $k-1$ between the reflector j and Rx, and ΔA is the reflective area.

C. Receiver

According to the scheme mentioned at the beginning of this Section, the optical receiver is made up of three main blocks, as can be seen in Figure 2. In this sense, the main components of a VLC receiver are a PD, an analog-to-digital converter (ADC) and a signal demodulator.

Table I
SIMULATION PARAMETERS

Parameters	Values
Length	3 m
Width	3 m
Height	3 m
Power	1 Watt
Field of view (FOV)	85°
Aperture Diameter	0.03 m
Reflection Coefficient	0.6
Lambertian Index	1
Distance between transmitters	7 cm

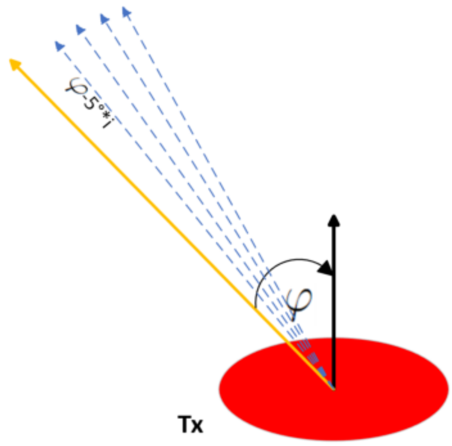

Figure 3. NLOS Rays from Tx.

III. PARAMETERS AND CHARACTERISTICS OF THE SIMULATION

This Section focuses on evaluating the performance of the proposed VLC system applied to an indoor environment that simulates a hospital scenario. This evaluation is carried out through computational simulations developed in MATLAB, integrating the characteristics of the designed components and the VLC channel. The characteristics and parameters used for the development of the simulations, together with their respective values and references, can be observed in Table I.

A. General Configuration of Transmission and Reception

Throughout all the tests conducted in the scenario, constant aspects were maintained in the simulations, such as the rays sent by the optical transmitter or how the optical receiver would receive the rays.

In the first case, the transmitter was configured to continuously generate a light beam directed directly at the optical receiver. Additionally, an NLOS beam was added, from which another ten beams were generated on the basis of this premise. However, only as a graphical reference, the first four beams are observed in Figure 3. In this Figure, we denote i as the number of the generated ray. As a second case, the optical transmitter was configured to emit a beam with two bounces, in which the second bounce, just like the rays from the optical transmitter in the first case, will be directed towards the receiver.

Regarding the receiver, it is simply evaluated whether the ray, after bounce, can impact PD, meeting the effective reception area based on the FOV, as can be seen in Figure 4.

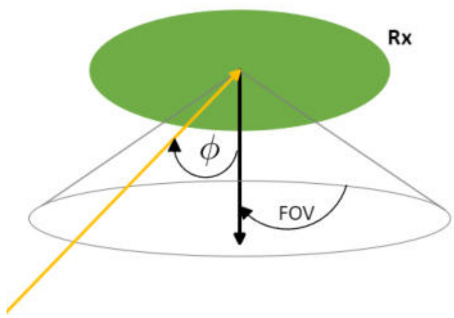

Figure 4. Reception of Rays in Rx.

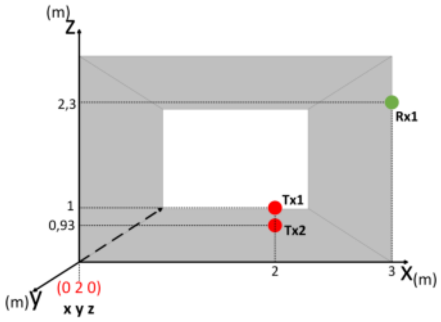

Figure 5. Sketch of the simulated scenario with points referencing the location of the LEDs and the PD.

B. General Configuration of the Scenario

To apply specific analysis cases in the simulated scenario, for simplicity and to establish a baseline for the study, it was decided to set the transmitter and receiver at the same coordinate on the y axis, as can be seen in Figure 5. In the referenced figure, the distance between the transmitters sketches their position on the bracelet, which could be optimized to improve its performance in future work. The positions of the transmitters for each case of the angles for the NLOS rays are described in Table II. To evaluate the results of the cases established in this scenario, the transmission of a binary code will be simulated, and it will be observed how the channel affects this message when it is received by the receiver. Moreover, one of the metrics chosen to evaluate the performance of the system is the CIR. To obtain various CIR curves, five different points in the scenario were evaluated and arbitrarily considered to focus the channel responses on distant points and observe the behavior of the graphs. These

Table II
POSITION OF SCENARIO ELEMENTS

Object	Parameters	Values
Tx1	Position Aiming Direction Irradiance Angle (φ_{NLOS})	(2,2,1)m (0,0,1) 65^o
Tx2	Position Aiming Direction Irradiance Angle (φ_{NLOS})	(2,2,0.93)m (0,0,-1) 40^o
Rx	Position Aiming Direction	(3,2,2.3)m (-3,0,-2)

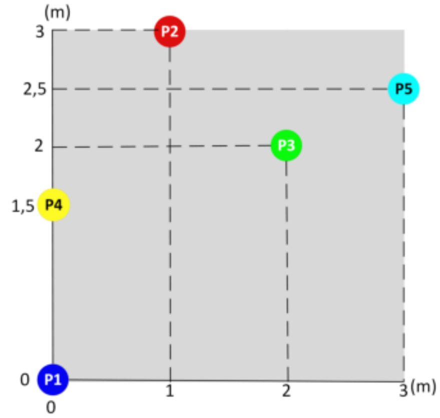

Figure 6. Reference points to obtain the CIR.

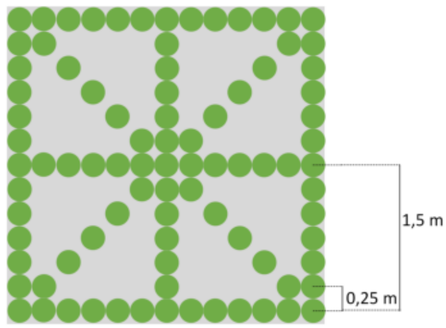

Figure 7. Reference points to obtain the CDF of the received power.

points can be seen as referenced in Figure 6 and correspond to positions P_1 (0,0,3), P_2 (1,3,3), P_3 (2,2,3), P_4 (0,1.5,3), P_5 (3,2.5,3), respectively. It should be noted that for visual and practical effects, Figure 6 is shown only in two dimensions, with the point (0,0,0) being the reference coordinate axis.

Finally, an important parameter that will allow for the verification of the system's performance is the received power, which will be presented as a CDF. To characterize the CDF, 49 points on the ceiling were evaluated and the maximum powers measured at those points were verified. In Figure 7, the reference points and the distance of 0.25 m chosen as the separation between the center of each point are shown.

IV. Analysis and Discussion of the Results

In this section, the performance of the system is presented in the different cases and reference positions that were chosen, with the first case being a proposed scenario regarding the transmitter and receiver positions, and the second case involving measurements made for different reception points to evaluate the performance of the proposed configuration. As a binary test code, for both cases, the message 1011010, was sent, which can be observed in Figure 8. This message was chosen only for demonstration purposes.

A. First Case

Based on the reception of this binary code when passing through the VLC channel, a CIR is obtained, which can be

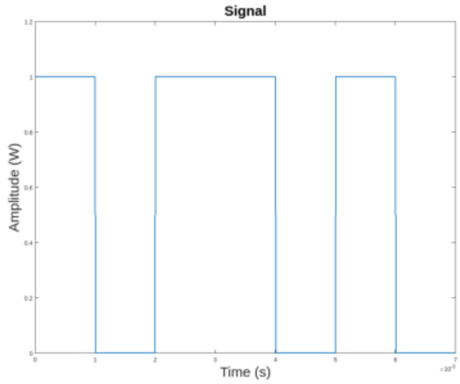

Figure 8. Modulated Test Binary Code

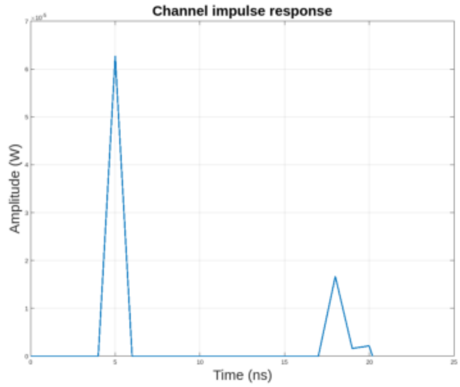

Figure 9. CIR Obtained from the First Simulation

seen in Figure 9. Here, we can observe the LOS component with greater magnitude and the NLOS components with a temporal delay and lesser magnitude.

According to Equation 1, when performing the convolution of the transmitted signal with the VLC channel, it can be observed that the signal is affected in amplitude and pulse width due to the influence of the channel. However, the message is still processed correctly, as can be seen in Figure 10.

The results obtained in this first case demonstrate that,

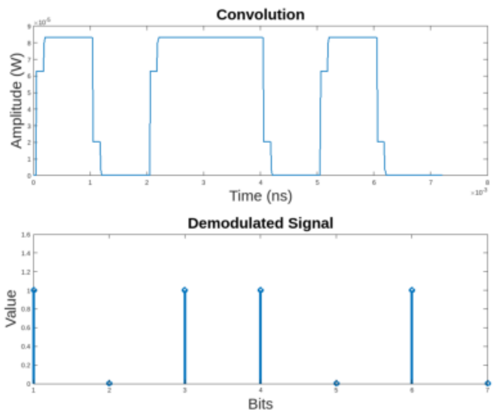

Figure 10. Results of the First Simulation

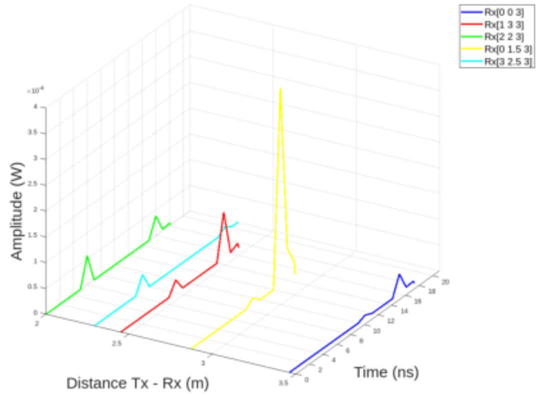

Figure 11. CIR Curves of Five Different Points in the Scenario.

within this scenario and with the conditions given in the simulation, the signal is not critically affected to the point of compromising the transmitted message. Therefore, within the ideal conditions proposed, there are still not enough obstacles or elements in the scenario that would degrade the signal and diminish the adequate performance of the developed system.

B. Second case

Considering the reference positions chosen in Section 3, a CIR curve was obtained for each point, which can be observed in Figure 11. This graph describes the five CIRs of the channel, taking into account the delays and arranging them according to the distance between the transmitter and the optical receiver.

The results obtained show a significant difference in the evaluation compared between different points. For example, at point P_4(0,1.5,3) a significantly higher maximum power is obtained compared to the rest of the evaluated points. This could be due to the simulated bounces, as these occur on the same wall where P_4 is positioned. Consequently, the peak of this CIR curve is in the NLOS components. Therefore, these are amplified and manage to generate significantly higher power than the rest of the maximum points evaluated in the CIR curves.

Finally, by obtaining the CDF of the power received for the 49 points at the ceiling of the scenario, the graph described in Figure 12 is obtained.

It can be seen in the CDF result that, in most of the points evaluated, the maximum power achieved in the sent pulses is usually not greater than 4×10^{-4} W. This result can be attributed to the simulated bounces, as they only bounce off one wall. Indeed, the higher probability is that the lower powers are related to the distance between the transmitter and the receiver along with the absence of the LOS component or the few NLOS rays that reach the receiver at the same delay.

An important detail to analyze and mention is the highest power obtained among the 49 measured points, which can be observed in Figure 13. This power occurs at the point (0,2,3), which is located at the same y coordinate as the transmitter, and, the receiver, is located next to the wall to which all the simulated NLOS rays are applied. This condition implies achieving an effect similar to that seen in Figure 11, where the best CIR curve is obtained by the accumulation of NLOS rays

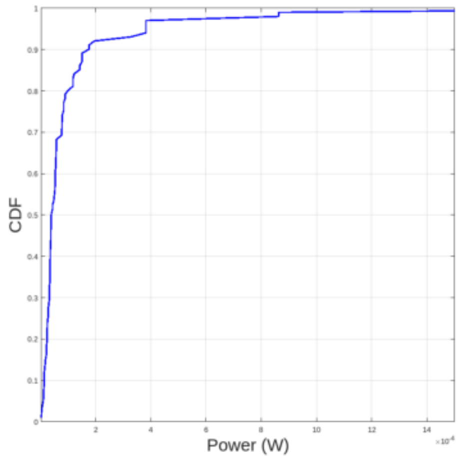

Figure 12. CDF of the Received Power

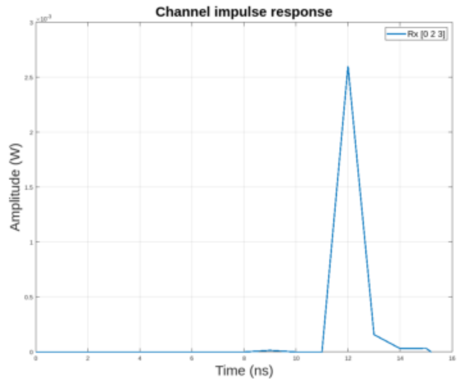

Figure 13. CIR of the point where the highest power was obtained

on a wall and at a distance similar to that from the bounce point to the receiver.

V. Conclusions and Future Considerations

This paper has provided an exploratory basis for the importance of efficient communication systems in the context of patient monitoring in hospital environments using VLC. Throughout the article, various aspects regarding patient monitoring have been proposed, highlighting the errors that a message can undergo when affected by different elements of the scenario, such as patient movement or obstacles that may exist between the transmitter and receiver. As a result of this research, a new transmitter has been proposed for these types of environment, along with evaluating channel performance when considering NLOS elements in the transmission channel.

The validation of the proposed system has been carried out under a simulation environment, which allows varying the distribution of VLC receivers in a hospital environment, similar to a patient's room, and verifying the variations that a message can have. The results obtained suggest a clear existence of optimal points when considering the proposed rays, Furthermore, due to the distance and the effects of the channel, there are no significant modifications in the data transmission that would distort the message being transmitted.

In general, the proposed system shows significant potential for patient monitoring in hospital settings. As progress is made in this line of research, it will be essential to refine the proposed model and consider additional characteristics of hospitals and data transmission via light. Variables such as interference from other electronic devices, the presence of temporary obstacles, and the variability of the arrangement of patients and medical staff, along with more NLOS rays that could compromise the integrity of the message to be transmitted, could be considered.

Acknowledgements

This research was supported by FONDECYT Regular 1211132, FONDECYT Iniciación 11240799, FONDECYT Iniciación 11241221, ANID PFCHA/Beca de Doctorado Nacional/2019 (21190489), SENESCYT "Convocatoria abierta 2014-primera fase, (Acta CIBAE-023-2014)" and Escuela de Informática y Telecomunicaciones, Universidad Diego Portales; also by the CISTER Research Unit (UIDP/UIDB/04234/2020) through FCT/MCTES (Portuguese Foundation for Science and Technology) National Funds.

References

[1] T. Georghiou, C. Sherlaw-Johnson, E. Massou, S. Morris, N. E. Crellin, L. Herlitz, M. S. Sidhu, S. M. Tomini, C. Vindrola-Padros, H. Walton, and N. J. Fulop, "The impact of post-hospital remote monitoring of covid-19 patients using pulse oximetry: A national observational study using hospital activity data," *eClinicalMedicine*, vol. 48, 2022.

[2] K. J. Jones, G. Haynatzki, and L. Sabalka, "Evaluation of automated video monitoring to decrease the risk of unattended bed exits in small rural hospitals," *Journal of Patient Safety*, vol. 17, 2021.

[3] I. Zagan, V. G. Găitan, A. I. Petrariu, N. Iuga, and A. Brezulianu, "Design, fabrication, and testing of an iot healthcare cardiac monitoring device," *Computers*, vol. 9, 2020.

[4] A. Bushnag, "A wireless ecg monitoring and analysis system using the iot cloud," *Intelligent Automation and Soft Computing*, vol. 33, 2022.

[5] P. P. Játiva, C. A. Azurdia-Meza, I. Sánchez, F. Seguel, D. Zabala-Blanco, A. D. Firoozabadi, C. A. Gutiérrez, and I. Soto, "A vlc channel model for underground mining environments with scattering and shadowing," *IEEE Access*, vol. 8, pp. 185 445–185 464, 2020.

[6] P. Palacios Játiva, I. Sánchez, I. Soto, C. A. Azurdia-Meza, D. Zabala-Blanco, M. Ijaz, A. Dehghan Firoozabadi, and D. Plets, "A novel and adaptive angle diversity-based receiver for 6g underground mining vlc systems," *Entropy*, vol. 24, no. 11, p. 1507, 2022.

[7] S. M. Mana, P. Hellwig, J. Hilt, K. L. Bober, V. J. Hirmanova, P. Chvojka, R. Janca, and S. Zvanovec, "Lifi experiments in a hospital," vol. Part F174-OFC 2020. Optica Publishing Group, 2020, p. M3I.2.

[8] W. Ding, F. Yang, H. Yang, J. Wang, X. Wang, X. Zhang, and J. Song, "A hybrid power line and visible light communication system for indoor hospital applications," *Computers in Industry*, vol. 68, 2015.

[9] D. R. Dhatchayeny, S. Arya, and Y. H. Chung, "Infrared-based multiple-patient monitoring in indoor optical wireless healthcare systems," *IEEE Sensors Journal*, vol. 19, no. 14, pp. 5594–5599, 2019.

[10] A. Al-Qahtani, H. Al-Hajri, S. Al-Kuwari, N. Al-Yaarabi, A. Al-Hababi, E. Al-Kubaisi, A. Ahmed, M. Kashef, and Q. H. Abbasi, "A non-invasive remote health monitoring system using visible light communication," 2015.

[11] Z. Ghassemlooy, *Optical wireless communications : system and channel modelling with MATLAB*. Boca Raton, FL: CRC Press, 2018.

[12] P. Palacios Játiva, M. Román Cañizares, C. A. Azurdia-Meza, D. Zabala-Blanco, A. Dehghan Firoozabadi, F. Seguel, S. Montejo-Sánchez, and I. Soto, "Interference mitigation for visible light communications in underground mines using angle diversity receivers," *Sensors*, vol. 20, no. 2, 2020.

[13] P. P. Játiva, C. A. Azurdia-Meza, M. R. Cañizares, D. Zabala-Blanco, and S. Montejo-Sánchez, "Performance analysis of ofdm-based vlc schemes in nlos channels," in *2020 South American Colloquium on Visible Light Communications (SACVLC)*, 2020, pp. 1–6.

[14] S. E.-D. N. Mohamed, A. E.-N. A. Mohamed, F. E. A. El-Samie, and A. N. Z. Rashed, "Performance enhancement of im/dd optical wireless systems," *Photonic Network Communications*, vol. 36, pp. 114–127, 2018.